6th World Congress on Structural and Multidisciplinary Optimization
Rio de Janeiro, 30 May - 03 June 2005, Brazil

Efficient Optimal Design of Electromagnetic Actuators Using Space-Mapping

Laurentiu Encica[(1)], David Echeverria[(2)], Elena Lomonova[(1)], André Vandenput[(1)], Piet Hemker[(2)], Domenico Lahaye[(2)]

[(1)]Eindhoven University of Technology, Eindhoven, The Netherlands,
Email: {L.Encica, E.Lomonova, A.J.A.Vandenput}@tue.nl
[(2)]Centre for Mathematics and Computer Science, Amsterdam, The Netherlands,
Email: {D.Echeverria, P.W.Hemker, D.Lahaye}@cwi.nl

1. Abstract
Engineering optimization procedures employ highly accurate numerical models that typically have an excessive computational cost, e.g. finite elements (FE). The space mapping (SM) technique speeds up the minimization procedure by exploiting also simplified (less accurate) models. We will use the SM terminology of fine and coarse in order to refer to the accurate and inaccurate models, respectively. SM implementation in the field of electromagnetic actuators design, in the context of constrained optimization, is a rather unexplored topic. A linear voice coil actuator is chosen as a benchmark test example. The key element in SM is the so-called SM function, which efficiently corrects the imprecise results that can be obtained with just coarse information. SM is used to solve a shape optimization problem. The design problem is stated as a minimization in which the computational cost lies completely in the constraint evaluation, thus SM is applied only to the constraints. A mathematical description of the approach is presented in this paper and two implementations are compared. The solution of the SM optimization is validated (locally) by means of a standard minimization routine. The numerical results obtained show a high efficiency of the SM-based optimization algorithm, reflected by a significantly low number of fine model simulations and an overall low computational effort.

2. Keywords: linear electromagnetic actuators, optimal design, space mapping, finite elements, equivalent circuits.

3. Introduction
The efficiency of electromagnetic actuators or their manufacturing and exploitation costs can be ameliorated by defining an optimal design problem [7]. In the majority of the situations, the practical technical requirements give rise to constrained, nonlinear optimization problems. In this paper we will consider the case of a single-objective, constrained optimization problem which is generally defined by

$$\min\left\{ f(\mathbf{x}) \middle| \mathbf{k}_{inq}(\mathbf{x}) \le 0, \mathbf{k}_{eq}(\mathbf{x}) = 0, \mathbf{A}\cdot\mathbf{x}' \le \mathbf{b}, \mathbf{x} \in X \subset \mathbb{R}^n \right\}, \tag{1}$$

where $f(\mathbf{x})$ is the objective function, $\mathbf{x}$ is the vector of design variables, and a set of linear and nonlinear (equality and inequality) constraints is given by $\mathbf{A}\cdot\mathbf{x}' \le \mathbf{b}$ and $\mathbf{k}_{inq}(\mathbf{x}) \le 0$, $\mathbf{k}_{eq}(\mathbf{x}) = 0$, respectively.

The need for high solution accuracy requires complex numerical models, and a classical approach for the direct optimization of such a model is in general a time consuming process. Optimization methods that exploit function/model approximation(s) or multi-level techniques are preferred alternatives.

The SM technique [1], [2] was introduced as an efficient optimization tool in the area of microwave devices, and has been applied successfully for the design of electromagnetic systems in [4]. Following from the review of the state of the art of SM optimization [1], it can be concluded that the implementation in the field of electromagnetic actuator design, in the context of constrained optimization is a rather unexplored topic. SM solves efficiently the optimization problem in Eq.(1) by exploiting also simplified model(s). Such models can be given by analytical formulations, equivalent circuits, FE models with coarse discretizations or other numerical modeling techniques. While the evaluation of these auxiliary models is by far less expensive, a drawback is their lower accuracy. The misalignment between the fine (accurate, expensive) and coarse (inaccurate, inexpensive) models is corrected by the so-called SM function. The main idea of the SM algorithms revolves around the method by which a mapping between the two models can be approximated and exploited. The general SM concept is described in Section 4. From the existing algorithms, the aggressive space mapping (ASM) [1], [3], [4] is chosen as the core of the implementation used to solve the shape optimization problem of a cylindrical voice coil actuator. A description of the approach and the algorithm are presented in Section 5, and the numerical results are given in Section 6. In the same section a standard optimization technique is employed to validate numerically the (local) optimality of the SM solution. The observations and conclusions are discussed in Section 7 and 8, respectively.

4. SM concept
Consider an accurate model $\mathbf{f}: X \subset \mathbb{R}^n \to \mathbb{R}^m$, denoted as a fine model. The set of variables $\mathbf{x}^*$ that represents the solution of a given optimization problem is

$$\mathbf{x}^* = \arg\min_{\mathbf{x}\in X} \left\| \mathbf{f}(\mathbf{x}) - \mathbf{y} \right\| \tag{2}$$

where $\mathbf{y}$ is a vector of design specifications.

If solving the problem in Eq.(2) is considered too expensive, a standard approach is to introduce a cheaper model $\mathbf{c}(\mathbf{z}): Z \subset \mathbb{R}^n \to \mathbb{R}^m$, a coarse model, which is faster to evaluate but also less accurate. The problem

$$\mathbf{z}^* = \arg\min_{\mathbf{z}\in Z} \left\| \mathbf{c}(\mathbf{z}) - \mathbf{y} \right\| \tag{3}$$

is easy to solve, but $\mathbf{z}^*$ is likely to differ from $\mathbf{x}^*$. To compensate for the misalignment between the models, a mapping function $\mathbf{p}$, relating the fine and coarse model variables, is defined as

$$\mathbf{z} = \mathbf{p}(\mathbf{x}) , \tag{4}$$

such that

$$\mathbf{c}(\mathbf{p}(\mathbf{x})) \simeq \mathbf{f}(\mathbf{x}) \tag{5}$$

in a region of interest, and $\mathbf{c}(\mathbf{p}(\mathbf{x}))$ is considered a surrogate for the fine model.
The direct optimization of the fine model can be avoided and, instead, a solution

$$\mathbf{x}_{sm}^* \triangleq \mathbf{p}^{-1}(\mathbf{z}^*) , \tag{6}$$

is considered as a good estimate of $\mathbf{x}^*$, where $\mathbf{z}^*$ is the result of the coarse model optimization, Eq.(3), [5]. Or, in an alternative formulation, the SM solution is determined by solving the optimization problem of the surrogate model [1], given by

$$\mathbf{x}_{sm}^* = \arg\min_{\mathbf{x}\in X} \left\| \mathbf{c}(\mathbf{p}(\mathbf{x})) - \mathbf{y} \right\| . \tag{7}$$

The SM function is the key element of the SM idea and it is more generally defined by

$$\mathbf{p}(\mathbf{x}) = \arg\min_{\mathbf{z}\in Z} \left\| \mathbf{c}(\mathbf{z}) - \mathbf{f}(\mathbf{x}) \right\| , \tag{8}$$

i.e. for a given fine variables vector **x** the function **p** delivers the best coarse parameter **z** that yields a similar response. It is not a strict assumption to consider that the space mapping function yields a unique value. The problems arising from multiple solutions are in practice dealt with via regularization [9] (i.e. introducing a bias towards a particular solution). It should be noted that an evaluation of the space mapping function is as expensive as one of the fine model.

5. SM Applied to Constraint Optimization Problems

At first the SM theory is quite general and can be directly applied. For simplicity of notations we will consider only equality constraints at this moment. The extension for inequality constraints will be given at the end of the section. Using the previously introduced notations, the accurate optimization problem we want to solve is

$$\mathbf{x}^* = \arg\min_{\mathbf{x}\in \widehat{X}\subset X} \left\| \mathbf{f}(\mathbf{x}) - \mathbf{y} \right\| , \tag{9}$$

aided by the fast approximation

$$\mathbf{z}^* = \arg\min_{\mathbf{z}\in \widehat{Z}\subset Z} \left\| \mathbf{c}(\mathbf{z}) - \mathbf{y} \right\| . \tag{10}$$

SM aims at computing the solution

$$\mathbf{x}_{sm}^* = \arg\min_{\mathbf{x}\in \widehat{X}} \left\| \mathbf{c}(\mathbf{p}(\mathbf{x})) - \mathbf{y} \right\| \tag{11}$$

where, following from Eq.(8), $\mathbf{p} : \widehat{X} \to \widehat{Z}$ is given by

$$\mathbf{p}(\mathbf{x}) = \arg\min_{\mathbf{z}\in \widehat{Z}\subset Z} \left\| \mathbf{c}(\mathbf{z}) - \mathbf{f}(\mathbf{x}) \right\| . \tag{12}$$

The sets $\widehat{X}$ and $\widehat{Z}$ are defined as

$$\begin{aligned} \widehat{X} &= \left\{ \mathbf{x} \in X \,\middle|\, \mathbf{k}_f(\mathbf{x}) = 0 \right\} \\ \widehat{Z} &= \left\{ \mathbf{z} \in Z \,\middle|\, \mathbf{k}_c(\mathbf{z}) = 0 \right\} \end{aligned} , \tag{13}$$

where $\mathbf{k}_f : X \to \mathbb{R}^{m_k}$ and $\mathbf{k}_c : Z \to \mathbb{R}^{m_k}$ represent m_k (nonlinear) constraint functions. Consequently, we can write Eq.(9) and Eq.(10) as follows

$$\mathbf{x}^* = \arg\min_{\mathbf{x}\in X} \left\| \mathbf{f}(\mathbf{x}) - \mathbf{y} \right\| \text{ subject to } \mathbf{k}_f(\mathbf{x}) = 0 \tag{14}$$

and

$$\mathbf{z}^* = \arg\min_{\mathbf{z}\in Z} \left\| \mathbf{c}(\mathbf{z}) - \mathbf{y} \right\| \text{ subject to } \mathbf{k}_c(\mathbf{z}) = 0 . \tag{15}$$

We also assume that the fine constraints $\mathbf{k}_f$ are expensive to evaluate and that the coarse constraints $\mathbf{k}_c$ are a fast approximation of them. For the numerical example presented in Section 6, the values of the fine constraints are given by magnetic field quantities and magnetic forces computed with a FE model. The sets *X* and *Z* are commonly hyper-boxes in $\mathbb{R}^n$.

5.1. Two-SM Functions Approach

In many cases the models **f** and **c** are not closely related to their respective constraints. Thus, it has no much sense to try to align them simultaneously via the SM function. A better strategy is proposed in [5]. Two SM functions $\mathbf{p}_m : X \to Z$ and $\mathbf{p}_k : X \to Z$

can be introduced, and they concern the alignment of the models and the constraints, respectively:

$$\mathbf{p}_m(\mathbf{x}) = \arg\min_{\mathbf{z}\in Z} \left\| \mathbf{c}(\mathbf{z}) - \mathbf{f}(\mathbf{x}) \right\| \tag{16}$$

and

$$\mathbf{p}_k(\mathbf{x}) = \arg\min_{\mathbf{z}\in Z} \left\| \mathbf{k}_c(\mathbf{z}) - \mathbf{k}_f(\mathbf{x}) \right\| . \tag{17}$$

Further, the new SM solution is defined as

$$\mathbf{x}^*_{2sm} = \arg\min_{\mathbf{x}\in X} \left\| \mathbf{c}(\mathbf{p}_m(\mathbf{x})) - \mathbf{y} \right\| \text{ subject to } \mathbf{k}_c(\mathbf{p}_k(\mathbf{x})) = 0 . \tag{18}$$

5.2. Simplified Approach

In our particular case, presented in the next section, the fine model **f** will coincide with the coarse one **c**:

$$\mathbf{f}(\mathbf{x}) = \mathbf{c}(\mathbf{z}), \forall \mathbf{x} \in X , \tag{19}$$

thus the SM function $\mathbf{p}_m$ will be the identity. Moreover, since for our design the number of design variables is larger than the number of imposed constraints, $n > m_k$, it is also assumable that

$$\mathbf{k}_c(\mathbf{p}_k(\mathbf{x})) = \mathbf{k}_f(\mathbf{x}), \forall \mathbf{x} \in X . \tag{20}$$

Thus, we can compute $\mathbf{p}_k(\mathbf{x})$ by just solving the system from Eq.(20). Noticing that $\mathbf{p}_m$ is the identity, if we substitute Eq.(19) and Eq.(20) into Eq.(18) we find that $\mathbf{x}^*_{2sm} = \mathbf{x}^*$. Consequently we are able to obtain the fine optimum with the two-SM-functions approach. This method performs efficiently with practical design problems, as it will be shown later.

The fact that $n > m_k$ causes some implementation problems. The system in Eq.(20) is not expected to have a unique solution (multiple points in the design space *Z* fulfill the same constraints). In practice we have to select one solution every time we apply $\mathbf{p}_k$. There are many possible criteria for this purpose and in this paper the next two are suggested:

$$\mathbf{p}_{k1}(\mathbf{x}) = \arg\min_{\mathbf{z}\in Z} \left\| \mathbf{c}(\mathbf{z}) - \mathbf{y} \right\| \text{ subject to } \mathbf{k}_c(\mathbf{z}) = \mathbf{k}_f(\mathbf{x}) \tag{21}$$

and

$$\mathbf{p}_{k2}(\mathbf{x}) = \arg\min_{\mathbf{z}\in Z} \left\| \mathbf{c}(\mathbf{z}) - \mathbf{f}(\mathbf{x}) \right\| \text{ subject to } \mathbf{k}_c(\mathbf{z}) = \mathbf{k}_f(\mathbf{x}) . \tag{22}$$

In the first case the preferred solution is the closest to the specification **y**, and the second criterion is based on the proximity to the fine model response $\mathbf{f}(\mathbf{x})$. The corresponding SM solutions

$$\mathbf{x}^*_{2sm1} = \arg\min_{\mathbf{x}\in X} \left\| \mathbf{c}(\mathbf{x}) - \mathbf{y} \right\| \text{ subject to } \mathbf{k}_c(\mathbf{p}_{k1}(\mathbf{x})) = 0 \tag{23}$$

and

$$\mathbf{x}^*_{2sm2} = \arg\min_{\mathbf{x}\in X} \left\| \mathbf{c}(\mathbf{x}) - \mathbf{y} \right\| \text{ subject to } \mathbf{k}_c(\mathbf{p}_{k2}(\mathbf{x})) = 0 \tag{24}$$

coincide with the fine optimum $\mathbf{x}^*$ and can be computed efficiently.

In order to include also inequality constraints, the Eq.(23) and Eq.(24), which give the SM solution, are extended to

$$\mathbf{x}^*_{2sm1} = \arg\min_{\mathbf{x}\in X} \left\| \mathbf{c}(\mathbf{x}) - \mathbf{y} \right\| \text{ subject to } \mathbf{k}_{c\_eq}(\mathbf{p}_{k1}(\mathbf{x})) = 0, \mathbf{k}_{c\_inq}(\mathbf{p}_{k1}(\mathbf{x})) \le 0 \tag{25}$$

and

$$\mathbf{x}^*_{2sm2} = \arg\min_{\mathbf{x}\in X} \left\| \mathbf{c}(\mathbf{x}) - \mathbf{y} \right\| \text{ subject to } \mathbf{k}_{c\_eq}(\mathbf{p}_{k2}(\mathbf{x})) = 0, \mathbf{k}_{c\_inq}(\mathbf{p}_{k2}(\mathbf{x})) \le 0 . \tag{26}$$

where following from the definition of the SM function given in Section 4, $\mathbf{p}_{k1}$ and $\mathbf{p}_{k2}$ become

$$\mathbf{p}_{k1}(\mathbf{x}) = \arg\min_{\mathbf{z}\in Z} \left\| \mathbf{c}(\mathbf{z}) - \mathbf{y} \right\| \text{ subject to } \mathbf{k}_{c\_eq}(\mathbf{z}) = \mathbf{k}_{f\_eq}(\mathbf{x}), \mathbf{k}_{c\_inq}(\mathbf{z}) = \mathbf{k}_{f\_inq}(\mathbf{x}) \tag{27}$$

and

$$\mathbf{p}_{k2}(\mathbf{x}) = \arg\min_{\mathbf{z}\in Z} \left\| \mathbf{c}(\mathbf{z}) - \mathbf{f}(\mathbf{x}) \right\| \text{ subject to } \mathbf{k}_{c\_eq}(\mathbf{z}) = \mathbf{k}_{f\_eq}(\mathbf{x}), \mathbf{k}_{c\_inq}(\mathbf{z}) = \mathbf{k}_{f\_inq}(\mathbf{x}) . \tag{28}$$

5.3. SM Algorithm

The core of the algorithm is the ASM method. At each iteration the SM function is approximated by a local linearization around the current point in the *X* design space. A trust region methodology is included to insure the overall robustness of the algorithm [1], [6]. The linear approximation of the SM function is considered valid only in a reduced region around the current point and the dimensions of the trust region are modified dependent on the quality of the approximation. A strategy to modify the trust region sizes is found in [6]. It is also implemented for our numerical trials, and the SM optimization routine has the following structure:

Step 1:

Solve the coarse model optimization to obtain

$$\mathbf{z}^* = \arg\min_{\mathbf{z}\in Z} \left\| \mathbf{c}(\mathbf{z}) - \mathbf{y} \right\| \text{ subject to } \mathbf{k}_{c\_eq}(\mathbf{z}) = 0, \mathbf{k}_{c\_inq}(\mathbf{z}) \le 0, \mathbf{A}\cdot\mathbf{z}' \le \mathbf{b} . \tag{29}$$

Since this not an expensive model, the optimization problem can be easily solved by means of a classical optimization technique.

Step 2:

Set $\mathbf{x}_1 = \mathbf{z}^*$ and verify the response of the fine model. If the constraints $\mathbf{k}_f$ are not satisfied within a predefined tolerance interval go to Step 3.

Step 3:

Initialize $i = 1$, $\mathbf{B}_i = \mathbf{I}$ (the identity matrix) and the trust region size $\boldsymbol{\delta}_i$.

Solve a coarse model parameter extraction (PE) to evaluate the misalignment between the two models (equivalent to an evaluation of the SM function for the current point in the *X* design space). One of the approaches in Eq.(27) or Eq.(28) can be used.

Initialize the residual vector

$$\mathbf{r}(\mathbf{x}_i) = \mathbf{p}_k(\mathbf{x}_i) - \mathbf{z}^* \tag{30}$$

that gives the measure of the distance between the current point in the *Z* design space and the coarse optimum.

Step 4:

Set the linear approximation of the SM function around the current point $\mathbf{x}_i$:

$$\mathbf{p}_k^{(i)}(\mathbf{x}) = \mathbf{p}_k(\mathbf{x}_i) + \mathbf{B}_i \cdot (\mathbf{x} - \mathbf{x}_i) \tag{31}$$

where $\mathbf{B}_i$ is the approximation to the Jacobian of $\mathbf{r}$ with respect to $\mathbf{x}_i$.

Step 6:

Solve the optimization problem that follows from Eq.(25) or Eq.(26):

$$\mathbf{x}_{i+1} = \arg\min_{\mathbf{x} \in X} \left\| \mathbf{c}(\mathbf{x}) - \mathbf{y} \right\| \text{ subject to } \mathbf{k}_{c\_eq}(\mathbf{p}_k^{(i)}(\mathbf{x})) = 0, \mathbf{k}_{c\_inq}(\mathbf{p}_k^{(i)}(\mathbf{x})) \le 0, \mathbf{A} \cdot \mathbf{x}' \le \mathbf{b} \text{ and } \left\| \mathbf{x} - \mathbf{x}_i \right\| \le \boldsymbol{\delta}_i . \tag{32}$$

Verify the fine model response to $\mathbf{x}_{i+1}$ and if the fine constraints are fulfilled stop and set $x_{sm2}^* = x_{i+1}$. Else go further to Step 7.

Step 7:

Evaluate $\mathbf{p}_k(\mathbf{x}_{i+1})$ and compute $\mathbf{r}(\mathbf{x}_{i+1})$. Set $\mathbf{h}_i = \mathbf{x}_{i+1} - \mathbf{x}_i$ and update the matrix $\mathbf{B}$ using the Broyden formula [1]:

$$\mathbf{B}_{i+1} = \mathbf{B}_i + \frac{\mathbf{r}(\mathbf{x}_{i+1}) - \mathbf{r}(\mathbf{x}_i) - \mathbf{B}_i \mathbf{h}_i}{\mathbf{h}_i^T \mathbf{h}_i} \mathbf{h}_i^T . \tag{33}$$

Update the trust region parameter $\boldsymbol{\delta}_i$ as in [6], set $i = i + 1$ and go to Step 4.

6. SM Optimization of a Cylindrical Voice Coil Actuator

A cylindrical voice coil actuator (CVCA) is considered as a study example. Most VCAs are used in applications like computer peripheral memories, medical equipment, high-speed lens focusing, laser tools, servo valves, and gravity and vibration compensation. This type of actuators can provide a cogging-free force output directly proportional to the applied current and can move an inertial load at high accelerations.

The configuration and the geometrical design variables of the axial symmetric CVCA are shown in Figure 1. The left and right air-gaps, indicated by p_1 and p_2 have fixed values.

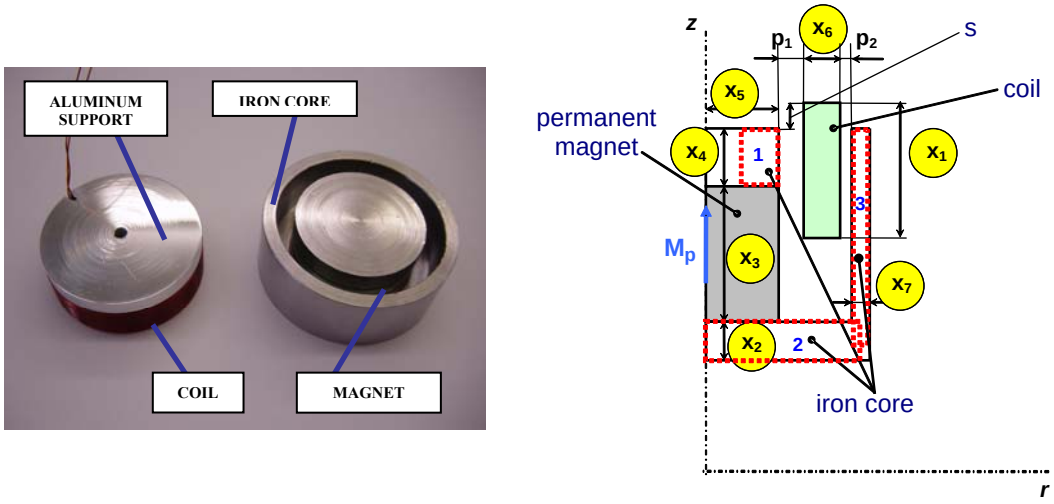

Figure 1. CVCA: geometrical configuration and design variables.

The actuator is composed of a static field assembly (an iron core and a NdFeB permanent magnet) and a moving coil for which a

constant level of the current density is defined. The position of the coil relative to the field assembly is indicated by the stroke *s*.
Two optimal design problems are presented and for both cases the two SM approaches indicates by Eq.(27) and Eq.(28) are tested. The goal of the optimal design problems is to determine the vector of design variables **x** that fulfils the following set of design specifications (the respective numerical values are later indicated for each example):

(a) minimizes the total mass of the actuator $M_t(\mathbf{x})$;

(b) a mass of the moving coil $M_c(\mathbf{x}) = M_0$;

(c) a force response at an indicated coil position $F(\mathbf{x})\big|_{s_0} = F_0$;

(d) a low level of the magnetic saturation in the iron core, estimated by the average values of the flux density in the three regions indicated in Figure 1: $B_{1,2,3}(\mathbf{x}) \le B_0$.

The maximum actuator stroke intervenes as a constraint in the design, thus a range of the stroke is introduced in the optimization problems as a set of linear inequality constraints:

$$s_{max} + s_{min} - x_1 + x_4 \le 0 \quad \text{and} \quad s_{min} + x_1 - x_3 - x_4 \le 0 \tag{34}$$

From the above list of design specifications the formulation of a single objective constrained optimization, which defines the fine model design problem, can be derived as follows:

$$\min\left\{ M_t(\mathbf{x}) \middle| B_{1,2,3}(\mathbf{x}) - B_0 \le 0, F(\mathbf{x})\big|_{s_0} - F_0 = 0, M_c(\mathbf{x}) - M_0 = 0, \mathbf{A}\cdot\mathbf{x}' \le \mathbf{b}, \mathbf{x} \in X \subset \mathbb{R}^n \right\}. \tag{35}$$

It can be observed that the difference between a fine and a coarse model will be found only in the force and flux density calculations, thus both fine and coarse design problems have the same objective function and are differentiated by the nonlinear constraints imposed on the force response and on the value of iron flux density. Similarly to Eq.(34), the auxiliary coarse model design problem is given by

$$\min\left\{ M_t(\mathbf{z}) \middle| B^c_{1,2,3}(\mathbf{z}) - B_0 \le 0, F^c(\mathbf{z})\big|_{s_0} - F_0 = 0, M_c(\mathbf{z}) - M_0 = 0, \mathbf{A}\cdot\mathbf{z}' \le \mathbf{b}, \mathbf{z} \in Z \subset \mathbb{R}^n \right\}. \tag{36}$$

6.1. Fine and Coarse Models

A. Fine model:
Considering the axial symmetry of the CVCA, a 2D FE model, that includes the nonlinear characteristics of the iron core, is chosen as a fine model. The implementation is realized with the Maxwell2D (Ansoft. Co.) software package.

B. Coarse model:
The principal requirement for a coarse model is a negligible calculation time. A magnetic equivalent circuit (MEC) of the CVCA is considered to be an appropriate choice. The model is built based on a set of simplifying assumptions:

(a) the iron core is considered linear, with a relative magnetic permeability $\mu_{rcore} = 1000$. The choice of this value is not arbitrary; it approximates the slope of the linear region of the BH curve for the type of material used in the FE simulations;

(b) the PM is considered linear and its relative recoil permeability μ_{rpm} is approximated to 1;

(c) the coil is not included in the equivalent circuit; consequently the effect of the coil current on the total field distribution is not accounted for; this assumption does not introduce a significant error because the PM has the dominant contribution to the magnetic field distribution in this system.

(d) the leakage magnetic fluxes are neglected.

The reluctance elements of an equivalent circuit model are calculated starting from the general expression

$$R = \frac{1}{\mu}\int_0^l \frac{dx}{A(x)}. \tag{37}$$

A flux tube (flux path) is characterized by the length *l*, the magnetic permeability μ, and the cross-section *A* which may vary with the length. Following from the simplifying assumptions the equivalent in from Figure 2 is derived.

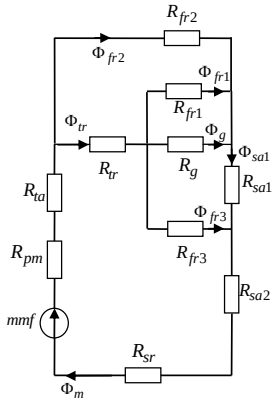

Figure 2. MEC model of the CVCA.

Detailed analysis of the MEC method and theory of the magnetic flux tubes can be found in [11], [12]. The PM is modeled as a magnetomotive force (*mmf*) source in series with a reluctance element R_m. The air gap magnetic flux distribution is modeled by one flux path Φ_g having radial direction, with the corresponding reluctance element R_g, and three additional flux tubes that model the fringing effects, $\Phi_{fr1,2,3}$. The lower part of the iron core (regions 2 and 3 in Figure 1) and the iron core tip are modeled by the circuit elements $R_{sa1,2}$, R_{sr}, and R_{ta}, R_{tr}, respectively. The main magnetic flux path is indicated by Φ_m.

A system of linear equations results from Kirchhoff's laws:

$$[A]\cdot[\Phi]=[f] \tag{38}$$

where $[A]$ is the coefficient matrix given by

$$[A]=\begin{bmatrix} 1 & -1 & 0 & 0 & -1 & 0 & 0 \\ 0 & 0 & 1 & 1 & 1 & 0 & -1 \\ -1 & 0 & 0 & 0 & 0 & 1 & 1 \\ R_{eqm} & 0 & 0 & 0 & R_{fr2} & 0 & R_{sa1} \\ R_{eqm} & R_{tr} & 0 & R_{fr1} & 0 & 0 & R_{sa1} \\ R_{eqm} & R_{tr} & R_g & 0 & 0 & 0 & R_{sa1} \\ R_{eqm} & R_{tr} & 0 & 0 & 0 & R_{fr3} & 0 \end{bmatrix} \tag{39}$$

and

$$R_{eqm}=R_{sr}+R_{pm}+R_{ta}+R_{sa2}\,. \tag{40}$$

The unknown magnetic fluxes are written in the column matrix

$$[\Phi]=\begin{bmatrix}\Phi_m & \Phi_{tr} & \Phi_g & \Phi_{fr1} & \Phi_{fr2} & \Phi_{fr3} & \Phi_{sa1}\end{bmatrix}^T \tag{41}$$

and the column vector $[f]$ is

$$[f]=\begin{bmatrix}0 & 0 & 0 & mmf & mmf & mmf & mmf\end{bmatrix}^T. \tag{42}$$

The system is solved for the magnetic fluxes, and the flux densities are calculated with

$$B_i=\frac{\Phi_i}{A_i}\,. \tag{43}$$

The force that acts on the coil, can be derived from Lorentz law

$$\mathbf{F}=\iiint_{V_c}\mathbf{J}\times\mathbf{B}dv\,, \tag{44}$$

where **J** is the coil current density, **B** is the magnetic flux density in the air gap and V_c is the volume of the coil. The resultant force will have only a *z* component since the radial component is canceled given the axial symmetry of the model.

6.2. Numerical Examples

The results of two numerical examples are detailed further. Each example is solved twice using the two SM approaches. We denote by SM1 the approach given by Eq.(25) and Eq.(27), and by SM2 the one given by Eq.(26) and Eq.(28).

The coarse model and the core of the SM optimization algorithm are implemented in Matlab's script language. An extra routine is written to allow for an automated interfacing between Matlab and Maxwell2D.

A global optimization procedure, DIRECT [8], in cascade with a sequential quadratic programming (SQP) algorithm [9], [10] are used to perform the optimization of the coarse model, the first step of the SM optimization (Section 5.3). Several trials indicated that the solution obtained is unique. The SQP routine only is applied in the PE and surrogate model optimization (Steps 3 and 6), where the starting points are the coarse optimum $\mathbf{z}^*$, for the first, and the current point in the *X* design space, $\mathbf{x}_i$ at the *i*-th iteration, for the second. The local optimality of the SM solution for the fine model is verified also with the SQP procedure.

The material properties and other parameters common to both examples are listed in Table 1 and Table 2. The design specifications for Example 1 together with the SM solution, the total calculation time, and the SQP solution are specified in Table 3.

Table 1. Material properties

	Coil	*Iron core*	*PM*
Mass density (kg/m^3)	8933	7872	7350
Current density (A/m^2)	$1.065\cdot10^7$	-	-
Remanent flux density B_r (T)	-	-	1.21
Relative permeability μ_r	1	BH nonlinear characteristic	1.04

The SM convergence history for the force response and one of the flux density responses are shown in Figure 3 and Figure 4, respectively. The tolerance criterion for the constraints is $\varepsilon=1e-3$. Figure 5 presents the flux density distribution calculated by FE for the

SM1 design solution. Following the same structure, the numerical results for Example 2 are indicated in Table 4 and Figures 6, 7 and 8.

Table 2. Other parameters

Parameters	Values
left air-gap p_1 *(mm)*	0.9
right air-gap p_2 *(mm)*	0.725
minimum stroke s_{min} *(mm)*	0.25
maximum stroke s_{max} *(mm)*	8.25

A. Example 1:

Table 3. Design specifications, coarse model optimal solution, SM fine model solution, SM computational effort and SQP solution

Design specifications	$B_{1,2,3} \le 1T,\ F = 5N\ \ at\ \ stroke\ \ s = 4.25mm,\ \ M_c = 10g$
$\mathbf{z}^*$ *(mm)*	[13.03231, 4.03140, 8.50000, 4.78231, 7.67098, 2.00878, 2.46469]
coarse model objective value M_t *(g)*	67.75543
$\mathbf{x}^*_{2sm1}$ *(mm)*	[11.70685, 3.46899, 8.50000, 3.45685, 9.90862, 1.82703, 2.44941]
SM1 objective value M_t *(g)*	80.27729
SM1 computational effort	5 iterations (5 FE simulations), 2.8 min.
$\mathbf{x}^*_{2sm2}$ *(mm)*	[11.70692, 3.46812, 8.50000, 3.45692, 9.90889, 1.82698, 2.44950]
SM2 objective value M_t *(g)*	80.27580
SM2 computational effort	5 iterations (5 FE simulations), 2.5 min.
$\mathbf{x}^*_{SQP}$ *(mm)*	[11.70942, 3.46651, 8.50000, 3.45942, 9.91051, 1.82639, 2.44946]

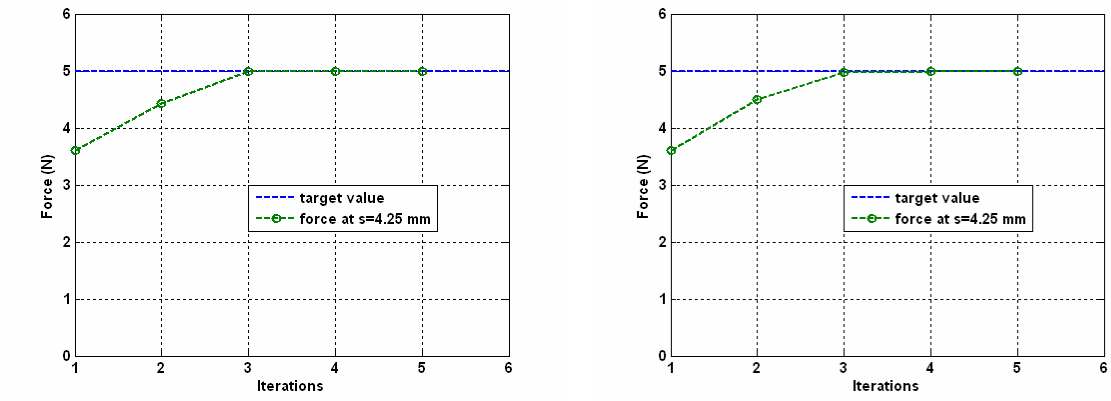

Figure 3. Convergence history of the fine model force response (Example 1): (a) SM1, (b) SM2.

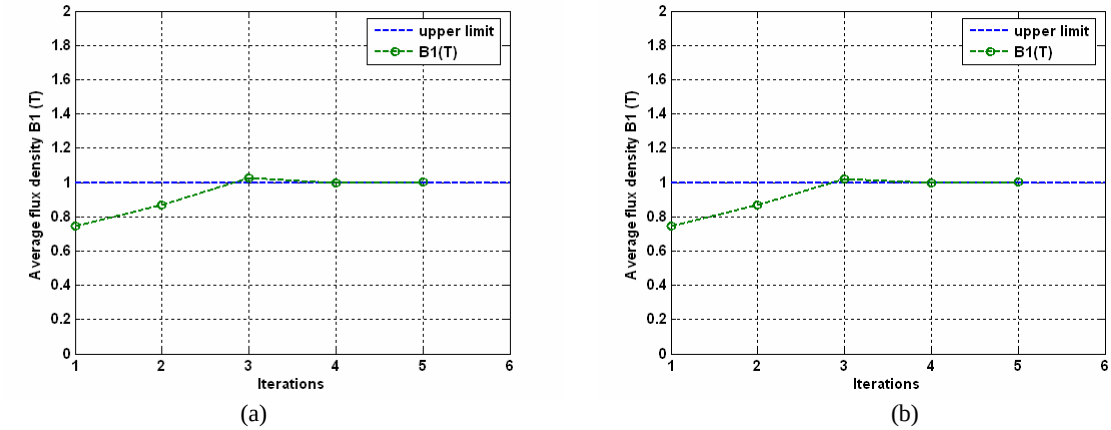

Figure 4. Convergence history of the fine model flux density B_1 (Example 1): (a) SM1, (b) SM2.

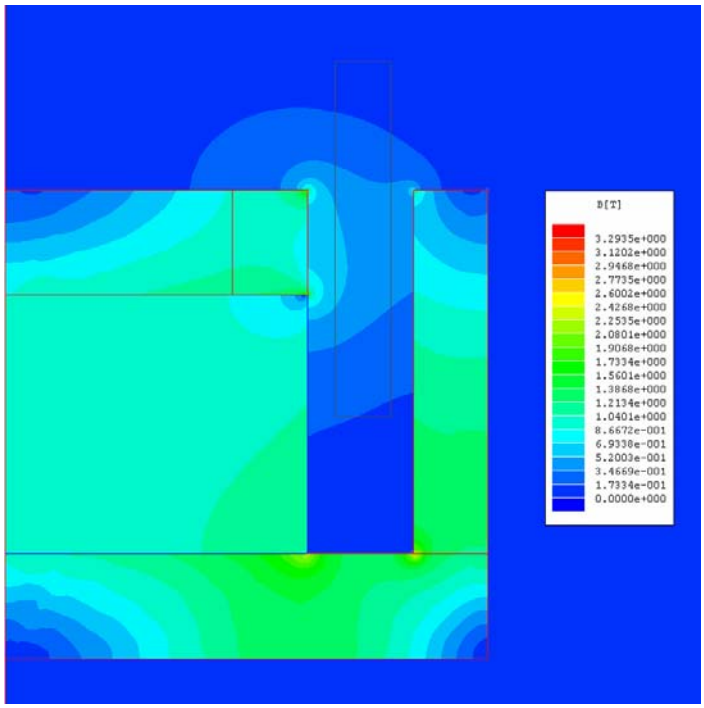

Figure 5. Flux density distribution calculated by FE for the SM1 solution (Example 1).

B. Example 2:

Table 4. Design specifications, coarse model optimal solution, SM fine model solution, SM computational effort and the SQP solution

Design specifications	$B_{1,2,3} \le 1T,\ F = 15N\ \ at\ \ stroke\ \ s = 4.25mm,\ M_c = 30g$
$\mathbf{z}^*$ *(mm)*	[15.17230, 5.25574, 9.16628, 6.25602, 10.43293, 3.75332, 3.15175]
coarse model objective value M_t *(g)*	158.49273
$\mathbf{x}^*_{2sm1}$ *(mm)*	[12.35562, 3.95932, 8.50000, 4.10562, 13.41786, 3.75928, 2.60098]
SM1 objective value M_t *(g)*	161.12988
SM1 computational effort	5 iterations (5 FE simulations), 2.9 min.
$\mathbf{x}^*_{2sm2}$ *(mm)*	[12.39704, 3.96632, 8.50000, 4.14704, 13.42534, 3.74647, 2.60873]
SM2 objective value M_t *(g)*	161.66620
SM2 computational effort	8 iterations (8 FE simulations), 4.1 min.
$\mathbf{x}^*_{SQP}$ *(mm)*	[12.35279, 3.96095, 8.50000, 4.10377, 13.40916, 3.74947, 2.60205]

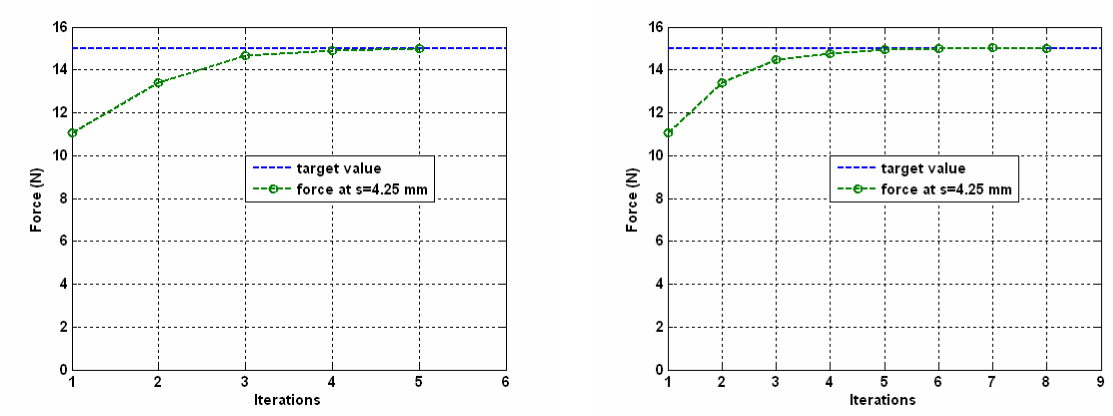

(a) (b)

Figure 6. Convergence history of the fine model force response (Example 2): (a) SM1, (b) SM2.

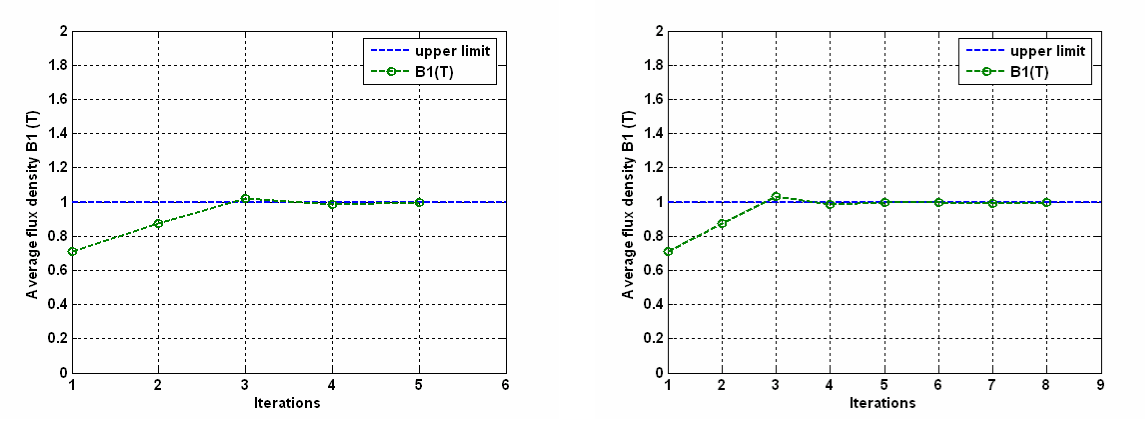

Figure 7. Convergence history of the fine model flux density B_1 (Example 2): (a) SM1, (b) SM2.

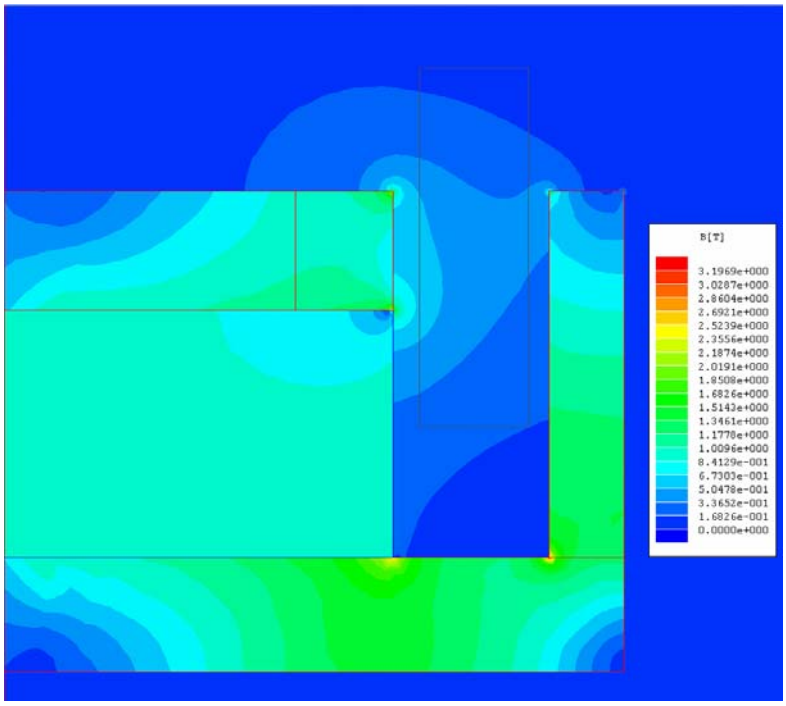

Figure 8. Flux density distribution calculated by FE for the SM1 solution (Example 2).

7. Observations

The two numerical examples indicate a high time efficiency of both SM implementations. Both algorithms are able to converge in a number of iterations that is smaller than/or comparable with the dimensions of the problem. The computational effort is given mainly by the fine model evaluations. The time needed for coarse model optimization(s) (Steps 1, 3 and 6) are basically negligible even when the number of coarse model evaluations goes up to several hundreds or even thousands. From the comparison of the two SM approaches it can be seen that both are able to find, within an interval of tolerance, the same optimal solution, which was also verified by the SQP routine. It can be observed, in the second example, that the SM2 approach shows a low oscillation before the error criterion is fulfilled, and more iterations are effectuated.

The option of using a coarse model based on a Maxwell2D FE model with coarse discretization was considered also. The computational time required was by far higher than the above presented implementation, and the study was not considered further. It still remains an open option, considering that a coarse FE model could provide a more flexible description of the physical phenomena than an equivalent circuit model.

8. Conclusions

The SM technique is regarded as a highly efficient tool for engineering optimization when expensive numerical models are necessary to describe the physical devices and phenomena. A mathematical overview of the basic concept of the technique is given and is then extended for constrained optimization problems, in particular for the case when only the constraints are functions expensive to evalu-

ate. We presented two SM approaches which return the same optimal solution with a low computational effort. The pairing between a FE fine model and a MEC coarse model seems to be an ideal choice for the optimal design of classical electric machinery and any other type of electromagnetic actuator that includes ferromagnetic core components as magnetic flux paths. For ironless/coreless actuators, different analytical/numerical modeling techniques can be used to define coarse models [13], [14].

9. Acknowledgment
This research is supported by the Dutch Ministry of Economic Affairs within the project IOP-EMVT 02201.

10. References

1. J.W. Bandler, Q.S. Cheng, S.A. Dakroury, A.S. Mohamed, M.H. Bakr, K. Madsen, and J. Sondergaard. Space Mapping: The State of the Art. IEEE Trans. Microwave Theory Tech., vol. 52, issue: 1, Jan. 2004, pp. 337 – 361
2. J. Bandler, R. Biernacki, S. Chen, P. Grobelny, and R. H. Hemmers. Space Mapping Technique for Electromagnetic Optimization. IEEE Trans. Microwave Theory Tech., 42 (1994), pp. 2536-2544
3. J. W. Bandler, R. M. Biernacki, S. H. Chen, R. H. Hemmers, and K. Madsen. Electromagnetic Optimization Exploiting Aggressive Space Mapping. IEEE MTT-S 1995 International Microwave Symposium, Orlando, Florida, (1995), pp. 1455-1458
4. H.S. Choi, D.H. Kim, I.H. Park, and S.Y. Hahn. A New Design Technique of Magnetic Systems Using Space Mapping Algorithm. IEEE Trans. Magn., vol. 37, issue: 5, Sept. 2001, pp. 3627 – 3630
5. S. J. Leary, A. Bhaskar, and A. J. Keane. A Constraint Mapping Approach to the Structural Optimization of an Expensive Model Using Surrogates. Optimization Eng., vol. 2, 2001, pp. 385–398
6. J. Sondergaard. Non-linear Optimization Using Space Mapping. Tech. Rep. IMM-EKS-1999-23, Danish Technical University, Lyngby, 1999
7. E. Fitan, F. Messine, and B. Nogarede. The Electromagnetic Actuator Design Problem: A General and Rational Approach. IEEE Trans. Magn., vol. 40, issue: 3, May 2004, pp.1579 – 1590
8. D.E. Finkel. DIRECT Optimization Algorithm User Guide. Centre for Research in Scientific Computation, North Carolina State University, CRSC-TR03-11, March 2003
9. P. Venkataraman. Applied optimization with Matlab programming. New York: Wiley-Interscience, 2002.
10. M.S. Bazaraa, H.D. Sherali, and C.M. Shetty. Nonlinear programming - theory and algorithms. 2nd ed. New York: Wiley-Interscience, 1993
11. H. C. Roters. Electromagnetic devices. New York: Wiley, 1941
12. V. Ostovici. Dynamics of saturated electric machines. Springer, 1989
13. D. Echeverria, D. Lahaye, L. Encica and P.W. Hemker. Optimization in Electromagnetics with the Space Mapping Technique. COMPEL The International Journal for Computation and Mathematics in Electrical and Electronic Engineering, Special Issue Volume 24, Issue 3, 2005
14. L. Encica, E.A. Lomonova, and A.J.A. Vandenput. A Study of the Space Mapping Approach to the Inverse Design Problem of a Coreless Actuator. Proc. of EPE-PEMC, 2004, Riga, Latvia